

# On the Limitations of the Color Dipole Picture

Carlo Ewerz<sup>a†</sup>, Andreas von Manteuffel<sup>b</sup>, Otto Nachtmann<sup>b</sup>

<sup>a</sup> ECT\*, Strada delle Tabarelle 286, I-38050 Villazzano (Trento), Italy

<sup>b</sup> Institut für Theoretische Physik, Universität Heidelberg, Philosophenweg 16,  
D-69120 Heidelberg, Germany

## Abstract

We discuss two aspects of the color dipole picture of high energy photon-proton scattering. First we present bounds on various ratios of deep inelastic structure functions resulting from the dipole picture that, together with the measured data, can be used to restrict the kinematical range of its applicability. The second issue that we address is the choice of energy variable in the dipole-proton cross section.

## 1 The dipole picture of high energy photon-proton scattering

The color dipole picture of high energy photon-proton scattering (or more generally photon-hadron scattering) [1, 2] has been a very popular and successful framework for the analysis of structure function data measured at HERA. In the dipole picture the photon-proton scattering is viewed as a two-step process. In the first step the real or virtual photon splits into a quark-antiquark pair – a color dipole – of size  $r = |\mathbf{r}|$  in the two-dimensional transverse plane of the reaction. The probability for this splitting to happen is encoded in the so-called photon wave function  $\psi_{T,L}^{(q)}(\alpha, \mathbf{r}, Q)$ , where  $Q^2$  is the photon virtuality,  $\alpha$  denotes the fraction of the longitudinal momentum of the photon that is carried by the quark, and  $q$  indicates the quark flavor. In leading order in the electromagnetic and strong coupling constants  $\alpha_{\text{em}}$  and  $\alpha_s$  the squared photon wave functions for transversely ( $T$ ) and longitudinally ( $L$ ) polarized photons are given by

$$\left| \psi_T^{(q)}(\alpha, \mathbf{r}, Q) \right|^2 = \frac{3}{2\pi^2} \alpha_{\text{em}} Q_q^2 \left\{ [\alpha^2 + (1 - \alpha)^2] \epsilon_q^2 [K_1(\epsilon_q r)]^2 + m_q^2 [K_0(\epsilon_q r)]^2 \right\} \quad (1)$$

and

$$\left| \psi_L^{(q)}(\alpha, \mathbf{r}, Q) \right|^2 = \frac{6}{\pi^2} \alpha_{\text{em}} Q_q^2 Q^2 [\alpha(1 - \alpha)]^2 [K_0(\epsilon_q r)]^2, \quad (2)$$

respectively. Here  $m_q$  is the quark mass for flavor  $q$ ,  $Q_q$  the corresponding electric charge, and  $\epsilon_q = \sqrt{\alpha(1 - \alpha)Q^2 + m_q^2}$ .  $K_{0,1}$  denote modified Bessel functions, and we have summed over the polarizations of the quark and antiquark. Integrating over the longitudinal momentum fraction  $\alpha$  we obtain a density for the photon wave function,

$$w_{T,L}^{(q)}(r, Q^2) = \int_0^1 d\alpha \left| \psi_{T,L}^{(q)}(\alpha, \mathbf{r}, Q) \right|^2. \quad (3)$$

---

<sup>†</sup> speaker at EDS07, Hamburg, May 2007

It gives the probability that a highly energetic, transversely or longitudinally polarized photon of virtuality  $Q^2$  splits into a quark-antiquark dipole of flavor  $q$  and size  $r$ .

In the second step of the reaction, the color dipole of size  $r$  scatters off the proton. Here the dipole is assumed to consist of an on-shell quark and antiquark and is treated as a hadron-like state. The second step is expressed in terms of the dipole-proton cross section  $\hat{\sigma}^{(q)}(r, W^2)$  which naturally depends on the quark flavor, the size of the dipole, and on the c.m.s. energy  $W$  of this subprocess. The two steps of the photon-proton reaction are then connected by integrating over the size and orientation of the intermediate dipole state and by summing over quark flavors to obtain the total  $\gamma^{(*)}p$  cross section,

$$\sigma_{T,L}(W^2, Q^2) = \sum_q \int d^2r w_{T,L}^{(q)}(r, Q^2) \hat{\sigma}^{(q)}(r, W^2). \quad (4)$$

In general, the dipole cross section  $\hat{\sigma}$  cannot be calculated from first principles. Instead, one uses models for  $\hat{\sigma}$  that implement certain features like saturation etc., and then fits the parameters of these models to measured data for the total structure function  $F_2$ , given for  $W^2 \gg Q^2$  and  $W^2 \gg m_p^2$  by  $F_2(W, Q^2) = Q^2[\sigma_T(W^2, Q^2) + \sigma_L(W^2, Q^2)]/(4\pi^2\alpha_{\text{em}})$ .

The dipole picture is not exact. Its derivation from a genuinely nonperturbative formulation of photon-proton scattering – or, in other words, its foundations in quantum field theory – have been studied in [3, 4]. As a key result of those papers the assumptions and approximations are spelled out in detail which are necessary to arrive at the usual dipole picture outlined above. In particular it was possible to identify correction terms which are potentially large in certain kinematical regions. As with any approximate formula it is important to determine as precisely as possible its range of applicability – in the case of the dipole picture the kinematical range in which potential corrections to the formulae given above are small. We will address this issue in the next two sections.

Note that the energy variable in the dipole-proton cross section  $\hat{\sigma}$  is  $W^2$ . However, many popular models for  $\hat{\sigma}$  use Bjorken- $x$ ,  $x = Q^2/(W^2 + Q^2)$ , instead. We will discuss the choice of energy variable in section 4 below.

## 2 Bound on $R = \sigma_L/\sigma_T$

The densities  $w_{T,L}$  are obviously non-negative (see (3)), and the same holds for the dipole cross sections  $\hat{\sigma}^{(q)}$ , since they are supposed to describe the physical scattering process of a dipole on a proton. We notice that in the formula (4) for the cross sections  $\sigma_L$  and  $\sigma_T$  the corresponding densities  $w_L^{(q)}$  and  $w_T^{(q)}$  are convoluted with the same dipole cross section  $\hat{\sigma}^{(q)}$ . Based on these observations one can derive bounds on the ratio  $R = \sigma_L/\sigma_T$  [4, 5] from the dipole picture. The ratio of two integrals with non-negative integrands cannot be smaller (larger) than the minimum (maximum) of the ratio of the integrands. Applied to the cross sections  $\sigma_L$  and  $\sigma_T$  of (4) this implies

$$\min_{q,r} \frac{w_L^{(q)}(r, Q^2)}{w_T^{(q)}(r, Q^2)} \leq R(W^2, Q^2) \leq \max_{q,r} \frac{w_L^{(q)}(r, Q^2)}{w_T^{(q)}(r, Q^2)}. \quad (5)$$

Note that here the dipole cross sections  $\hat{\sigma}^{(q)}$  drop out. Consequently, these bounds depend only on the well-known wave functions for longitudinally and transversely polarized photons. Let us

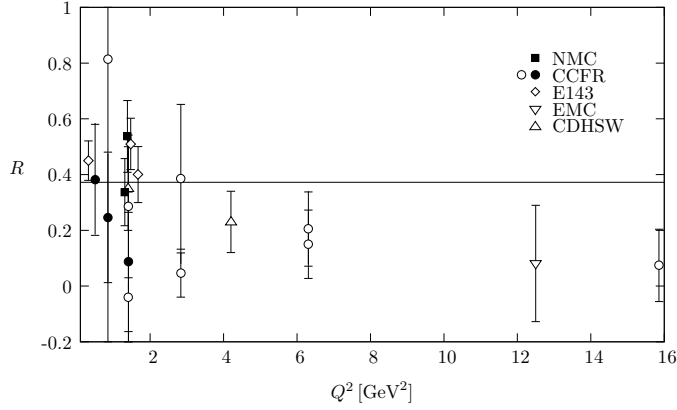


Fig. 1: Comparison of experimental data for  $R = \sigma_L/\sigma_T$  in the region  $x < 0.05$  with the bound (6) resulting from the dipole picture. Full points correspond to data with  $x < 0.01$ , open points are data with  $0.01 < x \leq 0.05$ .

point out that these bounds on  $R$  are independent of the choice of energy variable ( $W^2$  or  $x$ ) in the dipole cross section  $\hat{\sigma}$ . Evaluating the bounds (4) we find that the lower bound is trivial ( $R \geq 0$ ), and the upper bound has the numerical value

$$R(W^2, Q^2) \leq 0.37248. \quad (6)$$

This bound has to be satisfied in the kinematical region in which the dipole picture is applicable. A violation of the bound in some kinematical region, on the other hand, would indicate that the dipole picture cannot be used there.

The bound (6) is confronted with the experimental measurements of  $R$  in Fig. 1, where only data points with  $x < 0.05$  are included. The data have rather large error bars and seem to respect the bound. However, in the kinematical region of  $Q^2 < 2 \text{ GeV}^2$  the data appear to come very close to the bound – a situation that could hardly be accommodated with a realistic dipole cross section  $\hat{\sigma}$ . The application of the dipole picture in this interesting region (in which possible saturation effects are expected to become manifest) might therefore be questionable. Unfortunately, there are no HERA data on  $R$  available which could clarify this important point. For a detailed discussion and references to the corresponding experimental publications see [4,5].

### 3 Bounds on ratios of $F_2$ at different $Q^2$

In analogy to the derivation of the bound on  $R$  discussed above one can also obtain bounds on other ratios of deep inelastic structure functions. We can for example consider the ratio of structure functions  $F_2$  taken at the same energy  $W$  but at different photon virtualities  $Q^2$ . In [5,6] it was shown that for such a ratio one can derive the inequalities

$$\frac{Q_1^2}{Q_2^2} \min_{q,r} \frac{w_T^{(q)}(r, Q_1^2) + w_L^{(q)}(r, Q_1^2)}{w_T^{(q)}(r, Q_2^2) + w_L^{(q)}(r, Q_2^2)} \leq \frac{F_2(W, Q_1^2)}{F_2(W, Q_2^2)} \leq \frac{Q_1^2}{Q_2^2} \max_{q,r} \frac{w_T^{(q)}(r, Q_1^2) + w_L^{(q)}(r, Q_1^2)}{w_T^{(q)}(r, Q_2^2) + w_L^{(q)}(r, Q_2^2)}. \quad (7)$$

Note that for these bounds to be valid it is essential that the energy variable in the dipole cross section  $\hat{\sigma}$  is indeed  $W^2$ , in particular,  $\hat{\sigma}$  must not depend on  $Q^2$ . These bounds are independent

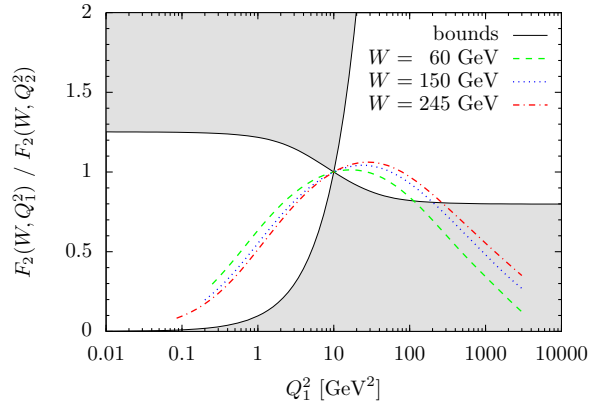


Fig. 2: The bounds (7) on  $F_2(W, Q_1^2)/F_2(W, Q_2^2)$  for  $Q_2^2 = 10 \text{ GeV}^2$  and the corresponding fit to HERA data for three different values of  $W$ . Data in the shaded region cannot be described in the usual dipole picture.

of any other assumptions about the dipole cross section  $\hat{\sigma}$ , and are in fact given in terms of the photon wave functions only. They also do not depend on the energy  $W$ .

In this case both the upper and the lower bound are non-trivial. Both bounds are shown in Fig. 2 for the choice  $Q_2^2 = 10 \text{ GeV}^2$ . In the dipole picture the shaded area is excluded. Also in that Figure we show the corresponding HERA data for three different energies  $W$ . More precisely, we show the ratios resulting from the ALLM97 fit [7] to the data. Within the experimental errors this fit can be regarded as a substitute of the data and is more convenient to use for a comparison with our bounds. (Note that we use this fit only within the kinematical range of the actual data.) As can be seen in the Figure the data violate the bound (7) at large  $Q^2$  while the bound is respected at low  $Q^2$ . We can therefore obtain a maximal photon virtuality  $Q_{\text{max}}^2$  beyond which the dipole picture breaks down. (In order to obtain an optimal value we have also varied the reference scale  $Q_2^2$ .) The  $W$ -dependence of this maximal  $Q^2$  is shown as the dashed line in Fig. 3. As expected, the dipole picture can be used up to higher  $Q^2$  for larger values of  $W$ .

In [6] we have considered correlated ratios of  $F_2$ -structure functions taken at the same energy  $W$  but at three different photon virtualities  $Q_i^2$ . It turns out that we can derive bounds on these correlated ratios from the dipole picture which are stronger than the bound discussed above. These bounds can be obtained from elementary geometrical considerations, but space limitations prevent us from presenting them here. We refer the interested reader to [6] for a detailed description. Using those methods we can show, for instance, that  $F_2(W, Q_1^2)/F_2(W, Q_3^2)$  is restricted to a certain range that in turn depends on the value of  $F_2(W, Q_2^2)/F_2(W, Q_3^2)$ . Also these correlated bounds do not involve any model assumptions about the dipole cross section  $\hat{\sigma}$  and are entirely given in terms of the photon wave functions. By confronting the correlated bounds with the ALLM97 fit to HERA data we have been able to restrict even further the range in  $Q^2$  allowed by the dipole picture. More precisely, we have obtained a  $Q_{\text{max}}^2$  up to which the three values  $Q_i^2$  can be chosen arbitrarily without giving rise to a violation of the bound by the corresponding data. In Fig. 3 the  $W$ -dependence of this  $Q_{\text{max}}^2$  is shown as the solid line. The correlated bounds give a stronger restriction on the kinematical range in which the dipole picture can be used as compared to the bound on the plain ratios (7).

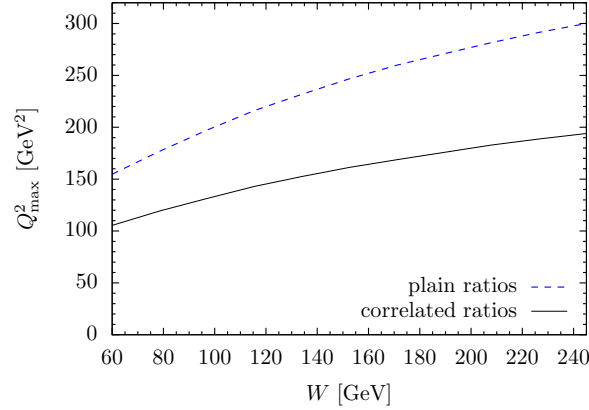


Fig. 3:  $W$ -dependence of the upper limit  $Q_{\max}^2$  of the  $Q^2$ -range in which the HERA data are consistent with the bounds obtained from the dipole picture. The dashed line results from the bound (7) while the solid line results from correlated bounds involving three different values of  $Q^2$ .

#### 4 The energy variable in the dipole cross section

Let us finally turn to the choice of energy variable in the dipole cross section  $\hat{\sigma}$ . Recall that the photon wave function describes the probability that a photon of virtuality  $Q^2$  splits into a dipole of size  $r$ . Clearly, for a given  $Q^2$  dipoles of all possible sizes  $r$  can emerge, with probabilities given by (1), (2) and (3). It is therefore not possible to extract  $Q^2$  from the dipole size  $r$ . Let us further recall that the second step of the scattering process in the dipole picture is the scattering of the dipole of size  $r$  on the proton. This dipole is fully characterized by  $r$  (and – less relevant here – its longitudinal momentum,  $\alpha$  and the spin orientations). The dipole-proton cross section  $\hat{\sigma}$ , understood as an actual scattering process of its own, can only depend on the properties of the initial state, namely the dipole and the proton. In particular, it cannot depend on the photon virtuality  $Q^2$ . Hence  $\hat{\sigma}$  cannot be a function of Bjorken- $x$  which can only be calculated with the knowledge of  $Q^2$ . For a more formal presentation of this argument see [4].

It is an interesting observation, on the other hand, that in the recent past almost all phenomenologically successful models for the dipole cross section use  $x$  as its energy variable. The most prominent example is the Golec-Biernat-Wüsthoff (GBW) model [8], for further references see [3, 4]. It is often argued that the probability distribution of dipole sizes has a maximum at  $r \simeq C/Q$  (where  $C \simeq 2.4$ ), and that therefore one can effectively replace the dipole size  $r$  in  $\hat{\sigma}$  by its most likely value. The value  $Q^2$  in  $x$  is then interpreted as corresponding to this most likely dipole size  $r$ ,  $Q = C/r$ . In Fig. 4 we have inverted this procedure for the case of the GBW model, that is we have reconstructed a  $W$ - but not  $Q^2$ -dependent  $\hat{\sigma}$  from its  $x$ -dependence. Here we plot again the ratio  $F_2(W, Q_1^2)/F_2(W, Q_2^2)$ , with the choice  $W = 60 \text{ GeV}$  and  $Q_2^2 = 10 \text{ GeV}^2$ , in order to compare with the bound (7). The effect of replacing  $Q \rightarrow C/r$  turns out to be sizable, especially at large  $Q^2$ . The modified model by construction respects the bound (7), while the original GBW model strongly violates it at large  $Q^2$ . The considerable difference between the two arises because the peak of the distribution of dipole sizes is actually rather broad, such that using only its maximum value is in fact not a good approximation.

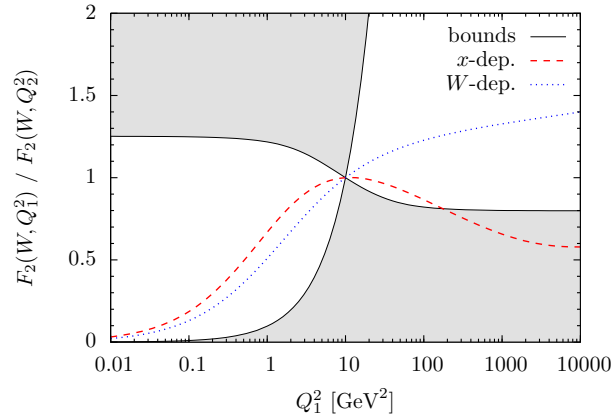


Fig. 4: Ratios of structure functions for the GBW model [8] ( $x$ -dependent dipole cross section, dashed line) and for a modification of the model with a  $W$ -dependent dipole cross section (dotted line) in comparison with the bounds (7).

Strictly speaking, the use of  $x$  instead of  $W$  in the dipole cross section is incorrect in the dipole picture. Phrased positively, it is actually a step *beyond* the dipole picture to use an  $x$ -dependent dipole cross section  $\hat{\sigma}$ . The better agreement of the  $x$ -dependent models of the dipole cross section with the data seems to indicate that some important corrections to the dipole picture are effectively taken into account by using  $x$  as the energy variable. In our opinion it would be very interesting to identify and to understand these additional contributions.

## 5 Conclusions

The dipole picture of high energy photon-proton scattering is only an approximation. We have derived various bounds on ratios of structure functions from the dipole picture, and have used these bounds to restrict the kinematical range of applicability of the dipole picture. One should analyse the data in the framework of the dipole picture only within this allowed range if one wants to arrive at firm conclusions. Further, we have discussed the choice of energy variable in models of the dipole cross section. We have pointed out that this issue is more delicate than has previously been assumed and certainly deserves to be studied in more detail.

## References

- [1] N. N. Nikolaev and B. G. Zakharov, Z. Phys. **C49**, 607 (1991).
- [2] A. H. Mueller, Nucl. Phys. **B415**, 373 (1994).
- [3] C. Ewerz and O. Nachtmann, Annals Phys. **322**, 1635 (2007). hep-ph/0404254.
- [4] C. Ewerz and O. Nachtmann, Annals Phys. **322**, 1670 (2007). hep-ph/0604087.
- [5] C. Ewerz and O. Nachtmann, Phys. Lett. **B648**, 279 (2007). hep-ph/0611076.
- [6] C. Ewerz, A. von Manteuffel, and O. Nachtmann (2007). arXiv:0708.3455 [hep-ph].
- [7] H. Abramowicz, E. M. Levin, A. Levy, and U. Maor, Phys. Lett. **B269**, 465 (1991);  
H. Abramowicz and A. Levy (1997). hep-ph/9712415.
- [8] K. Golec-Biernat and M. Wüsthoff, Phys. Rev. **D59**, 014017 (1999). hep-ph/9807513.